Biosensors and Bioelectronics 26 (2010) 1278–1282

Contents lists available at ScienceDirect

Biosensors and Bioelectronics

journal homepage: www.elsevier.com/locate/bios

Impedimetric immunosensor based on SWCNT-COOH modified gold microelectrodes for label-free detection of deep venous thrombosis biomarker

S. Bourigua[a,b], M. Hnaien[a], F. Bessueille[a], F. Lagarde[a], S. Dzyadevych[c], A. Maaref[b], J. Bausells[d], A. Errachid[a], N. Jaffrezic Renault[a,*]

[a] University of Lyon, Laboratory of Analytical Sciences, Claude Bernard University Lyon 1, 43 Boulevard 11 Novembre 1918, 69622 Villeurbanne Cedex, France
[b] University of Monastir, Laboratory of Physical and Chemistry of Interfaces, Faculty of Sciences of Monastir, Avenue of Environment, 5019 Monastir, Tunisia
[c] Laboratory of Biomolecular Electronics, Institute of Molecular Biology and Genetics, National Academy of Sciences of Ukraine, 150 Zabolotnogo St., Kiev 03143, Ukraine
[d] Centre Nacional de Microelectrònica (IMB-CSIC) Campus UAB, 08193 Bellaterra, Barcelona, Spain

ARTICLE INFO

Article history:
Received 8 April 2010
Received in revised form 1 July 2010
Accepted 2 July 2010
Available online 3 August 2010

Keywords:
Microelectrodes
Carbon nanotubes (SWNCT-COOH)
Electrochemical impedance spectroscopy
D-dimer

ABSTRACT

Measurement of D-dimer has subsequently become an essential element in the diagnostics of deep vein thrombosis and pulmonary embolism; in this context microelectrodes with an area of 9×10^{-4} cm^2 were used to develop impedimetric immunosensor for detecting deep venous thrombosis biomarker (D-dimer). The biosensor is based on functionalized carbon nanotubes (SWCNT-COOH) where the antibody (anti-D-dimer) was immobilized by covalent binding. The electrical properties and the morphology of the biolayer were characterized by electrochemical impedance spectroscopy (EIS), cyclic voltammetry and atomic force spectroscopy (AFM). Impedimetric microimmunosensor allows to obtain sensitivity of 40.1 kΩ μM^{-1} and detection limit of 0.1 pg/mL (0.53 fM) with linear range from 0.1 pg/mL to 2 μg/mL (0.53 fM to 0.01 μM). We demonstrate that using carbon nanotubes and microelectrodes, high sensitivity and dynamic range were obtained. The biosensor exhibited a short response time of 10 min. Moreover, the studied immunosensor exhibits good reproducibility (R.S.D. 8.2%, $n = 4$).

1. Introduction

In medicine, deep vein thrombosis (also known as deep venous thrombosis and usually abbreviated as DVT) is the formation of a blood clot in a deep vein. It is a form of thrombophlebitis (inflammation of a vein with clot formation) (Firkin and Nandurkar, 2009). A DVT can occur without any symptom, but in many cases the affected extremity will be painful, swollen, red, warm and the superficial veins may be engorged. The most serious complication of a DVT is that the clot could dislodge and travel to the lungs, which is called a pulmonary embolism (PE). DVT is a medical emergency, when present in the lower extremity, there is 3% chance of a PE killing the patient. The most commonly used tests for the diagnosis of DVT are a blood test called D-dimer test and Doppler ultrasound check-up of the affected veins (Spencer et al., 2007). D-dimer is a fibrin degradation product which contains two cross-linked D fragments of the fibrinogen protein. Its molar weight is around 190,000 g (Dempfle, 2006). Reference concentrations of plasma D-dimer (usually <0.50 μg/mL) are a useful negative predictor to rule out venous thromboembolism in patients (Bounameaux et al., 1994).

Immunosensor have a great interest with expectation of providing fast and highly sensitive immunological response (Park and Kim, 2006; Ramón-Azcón et al., 2008). During the past years, the research in this field has evolved quickly with the aim of improving the performance of the biosensors (specificity, stability, sensitivity, detection limit. . .) (Travas-Sejdic et al., 2006). In this approach, recent studies have focused on the miniaturization of system by the use of microelectrodes to develop microsensors and nanosensors.

Some of the most promising near term realizations of nanotechnology are at the interface of physical and biological system. Use properties and fabrication of these materials as nanosensors have been reported particularly for high-density arrays (Cui et al., 2001; Favier et al., 2001; Kong et al., 2000; Li et al., 2000). Hundreds of research articles using nanomaterials for electrochemical biosensing have been published since then. There are several reviews available which are based on electrochemical nanobiosensor (Wang, 2005; Jain, 2005; Patolsky et al., 2006; Pumera et al., 2007; Xiao and Li, 2008). Recently, Reshetilov and Bezborodov discussed the fundamental nature of interpenetration of nanotechnology and biosensor technology (Reshetilov and Bezborodov, 2008).

Carbon nanotubes (CNT) have become the focus of intensive research by analytical chemists (Iijima, 1991) for use in the functionalization of electrodes in order to amplify electrical signals of

* Corresponding author. Tel.: +33 472448306; fax: +33 472431206.
E-mail address: Nicole.jaffrezic@univ-lyon1.fr (N.J. Renault).

0956-5663/$ – see front matter © 2010 Elsevier B.V. All rights reserved.
doi:10.1016/j.bios.2010.07.004

the chemical and biological sensors (Wang, 2004; Merkoci, 2006). Fascinating physical and chemical properties such as electrical conductance, high mechanical stiffness, light weight and the possibilities of functionalizing CNTs to change their intrinsic properties are reasons for their use in the functionalization of novel biosensors (Gong et al., 2005; Veetil and Ye, 2008; Bustero et al., 2006). To use nanotubes in the functionalization of electrodes for electroanalytical purposes, proper conjugation strategies between biological molecules such as enzymes, single strand DNA/RNA/PNA, antibodies, receptors, and aptamers need to be developed.

In this paper, we developed an impedimetric immunosensor based on carbon nanotube (SWCNT-COOH) functionalized microelectrodes, in order to decrease the detection limit and increase the dynamic range compared to previous works where the detection limit was 0.1 ng/mL and the dynamic range was from 0.1 ng/mL to 10 ng/mL (Hafaid et al., 2010) which is out of the specifications of DVT diagnostics in terms of dynamic range.

2. Experiments

2.1. Reagents

The anti-D-dimer reduced antibody (Fab fragment hyst-ScAc) and the D-dimer antigen were obtained from Wyeth Company. Single-Walled Carbon Nanotubes (SWCNT-COOH) (ref DRP-CNT sol), were provided by DROPSENS, Spain. 11-amino-1-undecanthiol was obtained from Sigma Aldrich. N-(3-dimethylaminopropyl)-N′-ethyl-carbodiimide hydrochloride (EDC), N-hydroxysuccinidmide (NHS) and sodium dodecyl sulfate salt (SDS), used as surfactant was provided by Sigma–Aldrich.

The buffer solution used for all experiments was Phosphate Buffer Saline (PBS) pH 7.0. All solutions were made up in ultrapure water (resistance 18.2 MΩ cm^{-1}) produced by a Millipore Milli-Q system.

2.2. Fabrication of the microelectrodes based on silicon technology

The microelectronics fabrication process for the microelectrodes has been performed at Centro Nacional de Microelectronica (CNM). The process has only two photolithographic steps. The starting material is P-type ⟨1 0 0⟩ silicon 100 mm diameter wafers with a nominal thickness of 525 μm.

The process starts with a thermal oxidation process to grow a thick oxide layer (8000 Å). A first photoresist layer is then applied and patterned on the wafer surface. For a better adhesion of Au microelectrodes, a 10 nm Ti layer was introduced first, and then the 250 nm of Au layer was sputtered onto the surface. After that, photoresist layer was spin-coated and was exposed in UV light with a pattern mask. Etching away the exposed photoresist was performed, the left photoresist is exactly the microelectrodes, and then gold unprotected with photoresist was etched away. The next step consisted in the deposition of two PECVD (Plasma-Enhanced Chemical Vapor Deposition) layers of SiO_2 (4000 Å) and Si_3N_4 (4000 Å), acting as a passivation layer. The second photolithographic process was performed to open the passivation on the active Au microelectrodes (300 μm × 300 μm; area: 9×10^{-4} cm^2) and on the soldering pads (Marques de Oliveira et al., 2006a,b). The structure of the microelectrodes is shown schematically in Fig. 1.

2.3. Packaging of the microelectrodes

The wafer was diced and the devices were glued to a printed circuit board (PCB) and were wire-bonded in the usual manner. The bonding area of the devices, the bonding wires and the copper tracks of the PCB were then encapsulated using an epoxy resin (Epo-Tek H77, from Epoxy Technology) to protect them from the liquid environment.

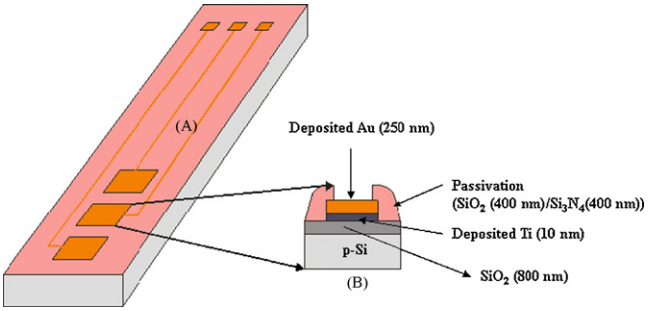

Fig. 1. (A) Schematic view of microelectrodes based on silicon technology; (B) Cross-section of one planar microelectrode.

2.4. Preparation of the immunosensor

2.4.1. Functionalization of the gold microelectrode with amino thiol

Before functionalization, the gold microelectrode was cleaned in an ultrasonic bath for 15 min in acetone and dried under a N_2 flow. Subsequently, the gold electrode was dipped for 1 min at room temperature in a piranha solution, and then rinsed with ethanol. Between and after these treatments, the gold microelectrodes were rinsed thoroughly with ultrapure water.

Subsequently, gold microelectrode was immersed in a solution of 11-amino-1-undecanethiol (amino thiol) 1 mM in ethanol solution for 5 h at 4 °C, in order to form a self-assembled monolayer (SAM). The substrate was then rinsed with ethanol to remove the unbonded thiols.

2.4.2. Covalent attachment of carbon nanotubes

Before carbon nanotubes immobilization, 0.17 g/L of the SWCNT-COOH material was dispersed in 0.1 mol/L aqueous solution of SDS. Then Single-Walled Carbon Nanotubes (SWCNT-COOH) were activated with a PBS solution containing 0.1 M NHS and 0.4 M EDC for 45 min, to convert the terminal carboxylic groups to an active NHS ester and then were maintained in contact with gold microelectrode functionalized with amino thiol for 2 h at room temperature. The substrate was then rinsed with ultrapure water.

2.4.3. Antibody immobilization

The active NHS ester functionalized carbon nanotubes SWNCT-COOH attached on gold microelectrodes were then maintained in contact with the anti-D-dimer reduced antibody for 1 h at room temperature. The excess antibodies were removed by rinsing with PBS.

2.4.4. Surface blocking with casein

The antibody-modified electrode was treated with a casein solution (50 mg/mL) for 30 min at room temperature, to block the unreacted and non-specific sites, and then the substrate was rinsed with PBS.

Then antigen solution with different concentrations was added and incubated on immobilized antibody for 10 min at room temperature.

2.5. Cyclic voltammetry

Cyclic voltammetry measurements were performed in a conventional three-electrode cell using a Voltalab 80, model PGZ 402,

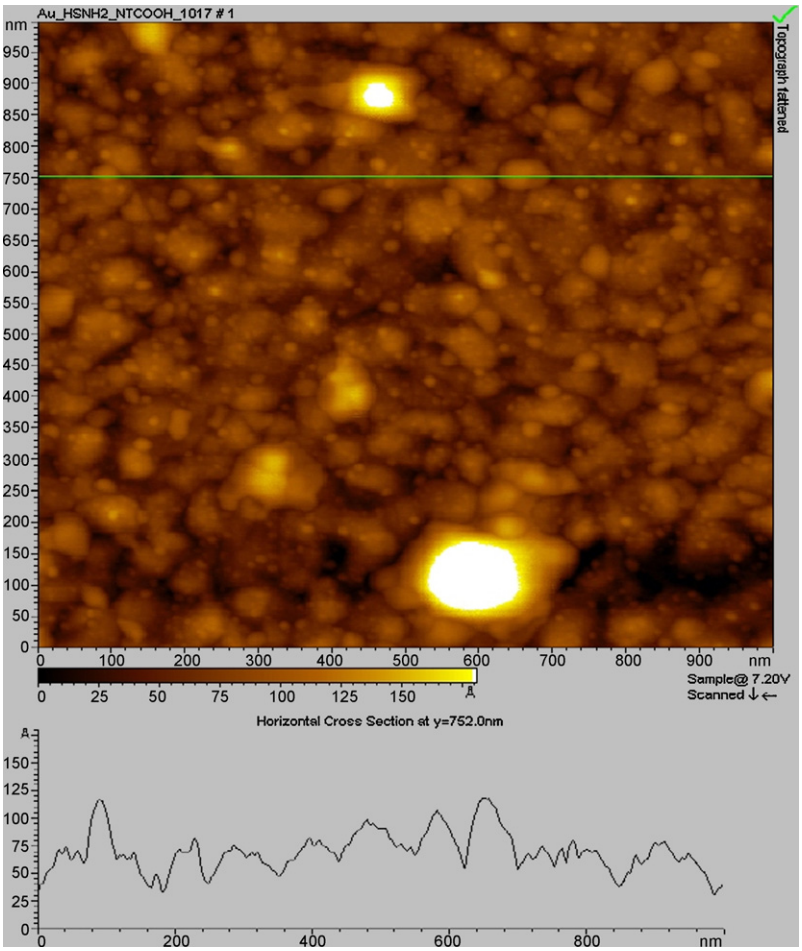

Fig. 2. AFM image of carbon nanotubes (SWCNT-COOH) fixed on amino-thiol functionalized gold electrode (1 μm × 1 μm).

controlled by software (Voltamaster 4) from Hach Lange France SAS, Marne-la Vallee.

Integrated microelectrodes with an area of 9×10^{-4} cm^2 based on gold were used as the working electrode. The reference electrode was a saturated calomel electrode (SCE). All potentials refered to this electrode (Biloivan et al., 2006; Marques de Oliveira et al., 2006a,b). The counter electrode was an integrated platinum microelectrode. The electrochemical measurements were performed in a 8 mM PBS buffer at pH 7.0 with 1 mM $Fe(CN)_6^{3/4-}$ at room temperature, 21 °C. A potential range of −0.5 to 0.7 V was applied with a scan rate of 100 mV/s.

2.6. Impedance spectroscopy

The electrochemical impedance measurements were performed using Voltalab 80, Model PGZ 402. The instrument was used in a three-electrode cell configuration as described before. The impedance spectroscopy measurements were carried out in the frequency range from 0.05 Hz to 100 kHz using a modulation voltage of 10 mV. Measurements were performed in a PBS buffer solution at pH 7.0. The measured impedance spectra were analyzed in terms of electrical equivalent circuits using the analysis program Zview (Scribner Associate Inc, Southern Pines, NC, USA).

2.7. Atomic force microscopy (AFM)

Atomic force microscopy (AFM) experiments were performed in air, using a Pico Plus Agilent/Scientec microscope with a 10 μm scanning head. The images were registered in "tapping" mode using silicon tips. The average resonance frequency of the tips was 300 kHz. The images presented in this paper were acquired with a resolution of 512 × 512 pixels and were processed by means of a plane fit. The scanned area size was 1 μm × 1 μm.

3. Results and discussion

3.1. Construction of the immunosensor and its characterization

The electrode modified with SWCNT-COOH wearing anti-D-dimer antibodies was analyzed by AFM to determine the efficiency of the covalent attachment. Fig. 2 shows the AFM image of functionalized gold with 11-amino-1-undecane thiol after carbon nanotubes immobilization. This image shows round globular particles with an average diameter of 75 nm corresponding to gold surface. A dispersion of nanoobjects of 15–20 nm of size is observed from reference Goh et al. (2009), when carbon nanotubes are dispersed in anionic surfactant SDS, SWCNT bundles are observed whose diameters are from 5 nm to 15 nm. The observed dimension would be the diameter of the SWCNT bundles. The length of SWCNT bundles is not observable due to the interaction of the tip with surface and to the initial roughness of gold electrode surface.

Modified electrode was electrochemically characterized in 8 mM phosphate buffer solution at pH 7.0 by cyclic voltammetry with 1 mM $Fe(CN_6)^{3/4-}$. The cyclic voltammograms show an increase in the current of oxidation–reduction peaks after carbon nanotube immobilization, indicating an increasing of electron transfer rate in presence of SWCNT-COOH.

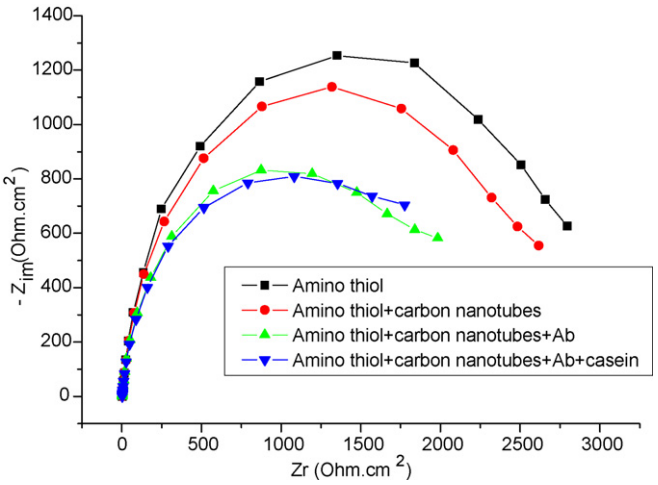

Fig. 3. Nyquist diagram ($-Z_{im}$ vs. Z_r) for the impedance measurements (at −0.5 V) vs. SCE in PBS solution (pH 7.0) corresponding to the various layers grafted onto the gold electrode: Spectra were obtained between 0.05 Hz and 100 KHz. Amplitude of alternative voltage: 10 mV.

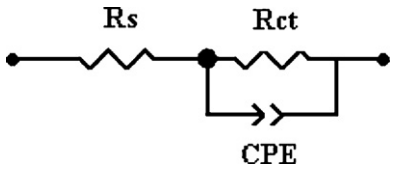

Fig. 4. Randles equivalent circuit of the SWCNT-COOH immunosensor.

In the second step, EIS was used in PBS (pH 7.0) at −500 mV potential in order to control the building-up of the biofilm. Fig. 3 shows the results of impedance spectroscopy measurements as Nyquist plots, for the assembly of the biofilm on gold electrode.

A decrease of the interfacial impedance is due to the attachment of carbon nanotubes on the aminothiol modified microelectrode. This decrease of the interfacial impedance proves that carbon nanotubes increase the conductivity of the electrode/electrolyte interface, due to their mixed metallic and P-type semiconducting properties, under −400 mV bias (Goh et al., 2009). Then the Nyquist plot shows a decrease of the interfacial impedance after antibody immobilization. The increase of CNT conductance was already observed after adsorption of negatively charged protein (Maehashi et al., 2007), these protein being placed inside the Debye length. In our case, the antibody used is in a reduced form, its small dimensions allow its location inside Debye length. A little increase of the interfacial impedance is observed after casein addition, due to the fact that the big size of casein could neutralize part of antibody effect. The impedance spectra were fitted with a simple Randles circuit, shown in Fig. 4 as recommended for nanocomposite materials thin films (Carrara et al., 2005). This equivalent electrical circuit consists of resistive and capacitive elements: R_S is the solution resistance, the constant phase element CPE is then

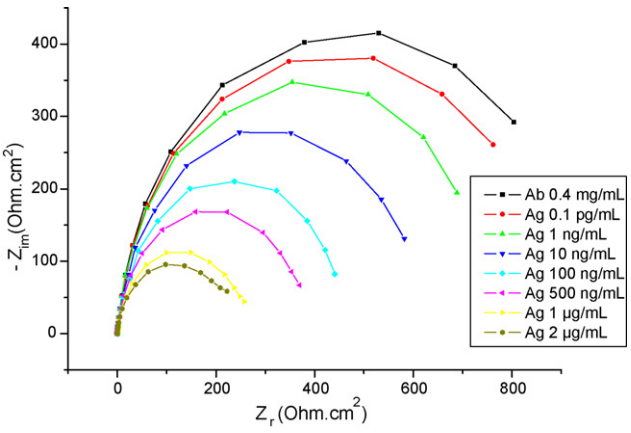

Fig. 5. Nyquist diagram ($-Z_{im}$ vs. Z_r) at −0.5 V vs.SCE in PBS solution pH 7.0) obtained for the impedance measurements on the SWCNT-COOH immunosensor under various concentrations of D-dimer. Spectra were obtained between 0.05 Hz and 100 KHz. Amplitude of alternative voltage: 10 mV.

related to the capacitance of the biofunctionalized SWCNT-COOH gold electrode/electrolyte interface. CPE reflects the non-ideality of the double-layer at the biofunctionalized SWCNT-COOH gold electrode/electrolyte interface due to the roughness and porosity of the biofilm. R_{ct} is related to the charge transfer resistance at the biofunctionalized SWCNT-COOH gold electrode/electrolyte interface. A good fitting was obtained as shown in Table 1 with a value of χ^2 of 0.002.

3.2. Response of the immunosensor to D-dimer

Before the immobilization of the antibody, the biosensor was tested by addition of antigen (D-dimer), no change in the impedance spectrum was observed.

Then the electrode modified with anti-D-dimer Antibody fragment was equilibrated with a range of concentrations of the specific antigen D-dimer from 0.1 pg/mL to 5 µg/mL (0.53 fM to 0.26 µM). Antigen–antibody interactions were monitored using impedance spectroscopy in PBS solution (pH 7.0).

The impedance spectra obtained after addition of different concentrations of antigen (D-dimer) are shown as Nyquist plots, in Fig. 5, where Z_r is the real part and Z_{im} is the imaginary part of the complex impedance Z. Immediately, at low frequencies, the impedance modulus $|Z(f)|$ decreases clearly with the increase of D-dimer concentration, which indicates that a larger amount of D-dimer interacts with the biofunctionalized surface. This reaction leads to a decrease in the electron transfer resistance. The increase of CNT conductivity could be explained by the increase of the negative charge of the immune complex which would induce an increase of CNT conductivity (Maehashi et al., 2007).

In order to quantify the immunosensor response, the calibration curves corresponding to the variation of the charge transfer resistance R_{ct} vs. concentrations of D-dimer in PBS solution, is presented

Table 1
Fitting parameters obtained from the Randles equivalent circuit of the SWCNT-COOH immunosensor.

Potentiel (mV)	Ag concentration	R_s (Ω cm^2)	R_{ct} (Ω cm^2)	CPE (mF cm^2)	α_{CPE}	χ^2
−500	0	19.68 ± 0.13	927.3 ± 1.82	0.17 ± 0.001	0.91 ± 0.0019	0.0019
	0.1 pg/ml	19.33 ± 0.12	872.4 ± 3.11	0.130 ± 0.002	0.88 ± 0.002	0.0018
	1 ng/ml	20.18 ± 0.13	768.6 ± 5.33	0.14 ± 0.002	0.89 ± 0.002	0.002
	10 ng/ml	20.91 ± 0.14	704.4 ± 8.66	0.097 ± 0.0003	0.86 ± 0.002	0.0017
	100 ng/ml	19.98 ± 0.12	661.9 ± 11.00	0.087 ± 0.0003	0.87 ± 0.002	0.0019
	500 ng/ml	20.90 ± 0.13	591 ± 15.26	0.082 ± 0.0005	0.86 ± 0.002	0.0021
	1 µg/ml	20.05 ± 0.13	479 ± 33.19	0.088 ± 0.0003	0.88 ± 0.002	0.0019
	2 µg/ml	20.67 ± 0.14	421 ± 12.12	0.089 ± 0.0005	0.86 ± 0.002	0.0020

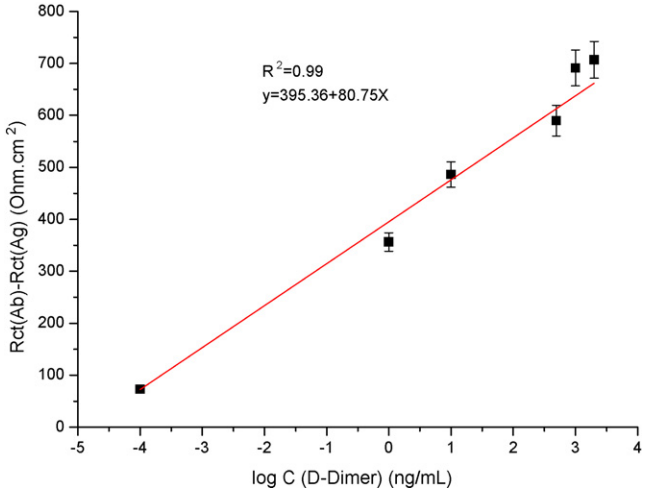

Fig. 6. Calibration curves describing the variation of charge transfer resistance ΔR_{ch} against logarithm of D-dimer concentration (C). (R.S.D. = 8.2%).

in Fig. 6. From the fitted data (Table 1), the immunosensor calibration curve presents a linear relation between R_{ct} and the logarithm of D-dimer concentration (C) ranging from 0.1 pg/mL to 2 μg/mL with a low detection limit of 0.1 pg/mL.

The results prove that the use of SWCNT-COOH modified microelectrodes lead to very interesting characteristics of the immunosensor such as limit of detection (0.1 pg/mL or 0.53 fM), linearity (up to 2 μg/mL or 0.01 μM), response time (10 min) and sensitivity (40.1 kΩ μM^{-1}); if we compare to the results obtained with polypyrrole modified macroelectrodes: detection limit (0.1 ng/mL or 0.53 pM), linearity (up to 10 ng/mL or 53 pM), response time (45 min) (Hafaid et al., 2010) and polypyrrole modified microelectrodes: detection limit (0.4 ng/mL or 2 pM), linearity (up to 0.4 μg/mL or 2 nM), response time (30 min) (Hafaiedh, 2009), we can deduce that the use of SWCNT-COOH modified microelectrodes lead to a 4000 times lower detection limit and a five times higher saturation limit. In the case of polypyrrole modified electrodes, the observed effect is an increase of R_{ct} when concentration of antigen increases. The effect has been attributed to a change in the electron conducting pathways brought by the formation of the immune complex (Sargent and Sadik, 1999).

For studying the repeatability of the immunosensor in PBS solution, we repeated this experience with four different immunosensors. A relative standard deviation of 8.2% was obtained what proves the reproducibility of the system.

The immunosensor was tested in heparinized rat blood spiked with 1 ng/mL (5.3 pM) of D-dimer. The impedance spectra obtained differ from those obtained in PBS of less than 10%. There was no detectable interference from heparinized rat blood components.

4. Conclusion

In this study, we have introduced a new method for the fabrication of a miniaturized impedimetric immunosensors for D-dimer detection, based on functionalized SWCNT-COOH modified microelectrodes ($S = 9 \times 10^{-4}$ cm^2). We have demonstrated that it is possible to improve specifications of the immunosensor in comparison to polypyrrole modified macroelectrodes. SWCNT-COOH immunosensors present a low limit of detection: 0.1 pg/mL (0.53 fM), a wide linear dynamic range (0.1 pg/mL–2 μg/mL or 0.53 fM–0.01 μM), a good sensitivity (40.1 kΩ μM^{-1}) and a short response time (10 min) and a good reproducibility (R.S.D. 8.2%, $n = 4$).

The SWCNT-COOH immunosensors present the required specifications for rapid tests for DVT diagnostics and will be inserted in point-of-care microsystems.

Acknowledgements

The authors thank EGIDE for support through UTIQUE programs 09G 1128 and 10G1103 and EC for support through NANOBIOSENS Project (PIRSES-GA-2008-2300802) and through DVT-IMP Project (FP6-IST- 34256). S. Bourigua thanks Rhone-Alpes Region for MIRA grant.

References

Biloivan, O.A., Verevka, S.V., Dzyadevych, S.V., Jaffrezic-Renault, N., Zine, N., Bausells, J., Samitier, J., Errachid, A., 2006. Materials Science and Engineering C 26, 574–577.
Bounameaux, H., de Moerloose, P., Perrier, A., Reber, G., 1994. Thrombosis and Haemostasis 71, 1–6.
Bustero, I., García, A., Obieta, I., Muñoz, R., Rincón, I., Arteche, A., 2006. Microchimica Acta 152, 239–247.
Carrara, S., Bavastrello, V., Ricci, D., Stura, E., Nicolini, C., 2005. Sensors and Actuators B 109, 221–226.
Cui, Y., Wei, Q., Park, H., Lieber, C.M., 2001. Science 293, 1289–1292.
Dempfle, C.-E., 2006. Thrombosis Research 118, 569–571.
Favier, F., Walter, E.C., Zach, M.P., Benter, T., Penner, R.M., 2001. Science 293, 2227–2231.
Firkin, F., Nandurkar, H., 2009. Australian Prescriber 32, 148–150.
Goh, R.G.S., Bell, J.M., Motta, N., Ho, P.K.-H., Waclawik, E.R., 2009. Superlattices and Microstructures 46, 347–356.
Gong, K., Yan, Y., Zhang, M., Su, L., Xiong, S., Mao, L., 2005. Analytical Sciences 21, 1383–1393.
Hafaiedh, I., 2009. Ph.D. Thesis #2009-ISAL-0052, INSA Lyon, France.
Hafaid, I., Chebil, S., Korri-Youssoufi, H., Bessueille, F., Errachid, A., Sassi, Z., Ali, Z., Abdelghani, A., Jaffrezic-Renault, N., 2010. Sensors and Actuators B 144, 323–331.
Iijima, S., 1991. Nature 354, 56–58.
Jain, K.K., 2005. Clinica Chimica Acta 358, 37–54.
Kong, J., Franklin, N.R., Zhou, C., Chapline, M.G., Peng, S., Cho, K., Dai, H., 2000. Science 287, 622–625.
Li, C.Z., He, H.X., Bogozi, A., Bunch, J.S., Tao, N.J., 2000. Applied Physics Letters 76, 1333–1335.
Maehashi, K., Katsura, T., Kerman, K., Takamura, Y., Matsumoto, K., Tamiya, E., 2007. Analytical Chemistry 79, 782–787.
Marques de Oliveira, I.A., Torrent-Burgués, J., Pla, M., Zine, N., Bausells, J., Escriche, Ll., Casabó, J., Errachid, A., Samitier, J., 2006a. Analytical Letters 39, 1709–1720.
Marques de Oliveira, I.A., Pla-Roca, M., Escriche, Ll., Casabo, J., Zine, N., Bausells, J., Teixidor, F., Crespo, E., Errachid, A., Samitier, J., 2006b. Electrochimica Acta 51, 5070–5074.
Merkoci, A., 2006. Microchimica Acta 152, 157–174.
Park, I.S., Kim, N., 2006. Analytica Chimica Acta 578, 19–24.
Patolsky, F., Zheng, G., Lieberet, C.M., 2006. Analytical Chemistry 78, 4260–4269.
Pumera, M., Sanchez, S., Ichinose, I., Tanget, J., 2007. Sensors and Actuators B 123, 1195–1205.
Ramón-Azcón, J., Valera, E., Rodríguez, Á., Barranco, A., Alfaro, B., Sanchez-Baeza, F., Marco, M.P., 2008. Biosensors and Bioelectronics 23, 1367–1373.
Reshetilov, A.N., Bezborodov, A.M., 2008. Applied Biochemistry and Microbiology 44, 1–5.
Sargent, A., Sadik, O.A., 1999. Electrochimica Acta 44, 4667–4675.
Spencer, F.A., Lessard, D., Emery, C., Reed, G., Goldberg, R.J., 2007. Archives of Internal Medicine 167, 1471–1475.
Travas-Sejdic, J., Peng, H., Cooney, R.P., Bowmaker, G.A., Cannell, M.B., Soeller, C., 2006. Current Applied Physics 6, 562–566.
Veetil, J.V., Ye, K., 2008. Biotechnology Progress 23, 517–531.
Wang, J., 2004. Electroanalysis 17, 7–14.
Wang, J., 2005. Analyst 130, 421–426.
Xiao, Y., Li, C.M., 2008. Electroanalysis 20, 648–662.